IEEE Access
Multidisciplinary | Rapid Review | Open Access Journal

Received September 29, 2019, accepted October 20, 2019, date of publication October 31, 2019,
date of current version November 13, 2019.

Digital Object Identifier 10.1109/ACCESS.2019.2950698

Adaptive Learning Gabor Filter for Finger-Vein Recognition

YAKUN ZHANG, WEIJUN LI, (Senior Member, IEEE), LIPING ZHANG, XIN NING, (Member, IEEE), LINJUN SUN, AND YAXUAN LU

Laboratory of Artificial Neural Networks and High-speed Circuits, Institute of Semiconductors, Chinese Academy of Sciences, Beijing 100083, China
Center of Materials Science and Optoelectronics Engineering, School of Microelectronics, University of Chinese Academy of Sciences, Beijing 100049, China
Cognitive Computing Technology Joint Laboratory, Wave Group, Beijing 100083, China

Corresponding authors: Weijun Li (wjli@semi.ac.cn) and Xin Ning (ningxin@semi.ac.cn)

This work was supported in part by the National Natural Science Foundation of China under Grant 61572458 and Grant 61901436.

ABSTRACT Presently, finger-vein recognition is a new research direction in the field of biometric recognition. The Gabor filter has been extensively used for finger-vein recognition; however, its parameters are difficult to adjust. To solve this problem, an adaptive-learning Gabor filter is presented herein. We combine convolutional neural networks with a Gabor filter to calculate the gradient of the Gabor-filter parameters, based on the objective function, and to then optimize its parameters via back-propagation. The parameter θ of Gabor filter can be trained to the same angle as the vein texture of finger vein image. The parameter σ of Gabor filter has a certain relation with λ, and the parameter λ of Gabor filter can converge to the optimal value well. Using this method, we not only select appropriate and effective Gabor filter parameters to design the filter banks, we also consider the relationship between those parameters. Finally, we perform experiments on four public finger-vein datasets. Experimental results demonstrate that our method outperforms state-of-the-art methods in finger-vein classification.

INDEX TERMS Gabor filters, vein recognition, convolutional nerual networks, adaptive learning.

I. INTRODUCTION

Finger-vein recognition is a new recognition technology of biometrics [1]. It mainly utilizes the absorption characteristics of near-infrared light caused by the hemoglobin in the finger veins, thereby collecting finger-vein images for identification [2]. Compared to fingerprint recognition and other biometric recognition [3], [4], finger-vein information is not easy to replicate. Therefore, finger-vein recognition is relatively safer and more stable than fingerprint recognition. However, owing to the influence of illumination and the complexity of finger veins, feature extraction of finger veins is difficult [5].

The classical feature extraction methods of finger-vein recognition are based on Fourier transform [6], local histogram and global histogram normalization [7], and sparse representation [8]. However, these methods provide trivial improvements to finger-vein recognition performance with low-quality finger-vein images. A filter with orientation has an obvious effect on the extraction of vein-texture information. For example, Wang *et al.* [9] proposed a new method for palm vein identification, based on Gabor wavelet filters to extract vein feature. Other researchers proposed image segmentation methods for finger veins, including the classical repetitive linear-tracking algorithm [10] and a series of improved methods. The Gabor filter is used for texture and orientation extraction. It is not only a common method for finger-vein image enhancement, but it is also a common method for extracting finger-vein texture features. Therefore, the Gabor filter plays an important role in finger-vein recognition technology. Yang et al. proposed a homomorphism filter and a Gabor filter [11], [12]. In terms of image enhancement and texture-feature extraction, Zhang and Yang [13] proposed a gray-level combination of the circular Gabor-filter enhancement method. Yang and Yang [14] proposed a multi-channel Gabor-filter enhancement method. Ferrer *et al.* [15] produced a template by filtering an extended infrared hand dorsum image with a Gabor filter. Shi and Yang [16] proposed an enhancement method, based on scatter removal and symmetric Gabor-filter banks. Xie *et al.* [17] proposed a method combining symmetric Gabor filter with a steering filter to extract the

The associate editor coordinating the review of this manuscript and approving it for publication was Chunbo Xiu.

finger-vein image. Lu *et al.* [18] proposed a feature extraction method based on Gabor-corresponding histograms. Yang et al. proposed the Gabor+Tri-branch structure [19] and point group method combined with a Gabor filter (PG-Gabor) [20] to utilize the vein point and non-vein point. These methods solve different problems in finger-vein recognition. Nevertheless, it is difficult to configure the parameters of the Gabor filter. In different applications and different datasets, one must manually adjust the parameters to find relative optimal value. This makes parameter-setting very difficult.

Furthermore, little attention has been paid to the importance of individual filters in a Gabor-filter bank. The current practice assumes that all filters of a filter bank are important. However, among the large number of filters in a Gabor-filter bank, only a subset are significant, whereas others are either redundant or irrelevant. To solve these problems, an adaptive-learning Gabor filter is proposed. The main contributions of this paper include:

1) Resolving the difficulty of configuring the parameters of the Gabor filter, improving the utilization ratio of the Gabor-filter bank for finger-vein recognition.
2) Providing a new solution for texture recognition by combining gradient descent and the convolution processing of a Gabor filter.

The rest of this paper is organized as follows: Section 2 introduces related work; Section 3 explains our method; Section 4 presents the experimental results of our method; Section 5 provides the findings and conclusion.

II. RELATED WORK

A. FINGER VEIN RECOGNITION METHODS

In recent years, many finger vein recognition methods have been proposed and applied. We classify the identification methods into two categories, one is the method of the non-deep neural network, the other is the method of deep neural network.

Non-deep neural network methods: Before the deep neural network method, there are many classical handcrafted feature extraction methods. Naoto Miura et al. proposed the methods of iteratively tracking local lines [21] and maximum curvature points [22] to extract the global vein veins, to solve the problem of unclear finger vein images caused by finger position changes and illumination problems. Eui Chul Lee *et al.* [23] proposed to represent veins by the minute nodes of finger veins, and use local binary pattern (LBP) to code finger veins to improve recognition performance. To solve some problems of LBP, researchers proposed LLBP (local line binary pattern) [24], ELBP (efficient local binary pattern) [25]. Based on the relationships among vein subjects, a novel discriminative binary codes (DBC) [26] learning method is proposed and proved to be effective. To learn a feature mapping relationship to enhance the recognition ability of local features, a discriminative binary descriptor (DBD) [27] method is proposed. Recently, there are some classical methods of encoding and extracting features, such as k-means hashing-based method (KMHM) [28], iterative quantization-based method (ITQM) [29], weighted vein code indexing [30], anatomy structure analysis-based vein extraction (ASVAE) [31].

Deep neural network methods: Wu and Ye [1] proposed using Radon transform to extract features of finger vein, and then using neural networks to classify. Radzi *et al.* [32] exploited a four-layer CNN to extract features and compared the Euclidean distance of features. And the latest methods of deep neural networks include light convolutional neural networks [33], two-stream convolutional neural networks [34] and fully convolution neural networks [35]. Qin and El-Yacoubi [36] proposed a deep representation based feature extraction method. Firstly, the foreground and background of the finger image were segmented to obtain the foreground segmentation image. Then, each pixel of the foreground segmentation image is predicted to be vein point or non-vein points using CNN. Finally, the missing vein pattern in the segmented image was recovered by a fully convolution neural network.

B. GABOR FUNCTION

The Gabor filter [37] is a type of wavelet. The one-dimensional (1D) form of the Gabor function was first proposed by the British physicist, Gabor, in 1946. Subsequently, Daugman [38] proposed a two-dimensional (2D) Gabor function in 1980. The Gabor filter has a good time-domain and frequency-domain transform characteristics. Gabor functions are used to construct filters with different scaling directions caused by different parameters (e.g., spatial position, frequency, phase, and direction). Furthermore, Marcelja [39] showed that 1D Gabor functions could well-describe simple cellular receptive fields. Daugman [38] conducted a 2D spectral analysis of the distribution of cortical receptive fields, and the research of [40] proved this relationship. Neurophysiological studies have shown that the spatial structure of receptive fields of simple cells of different sizes are actually the same. Daugman [41] and Porat and Zeevi [42] showed that all simple cells could be best modeled by a set of 2D Gabor wavelets, sampled in a logarithmic manner in the frequency domain.

Many experimental studies have shown that images can be divided into spatial and frequency-domain components for visual cortex perception. Furthermore, an image can be represented by locally symmetric and anti-symmetric base functions. The Gabor function has the same characteristics as the 2D reflex zone of simple cells in the human cerebral cortex. The Gabor function can capture local structure information corresponding to spatial frequency (scale), spatial location, and direction selectivity. Thus, the 2D Gabor filter matches the received field model of mammalian retinal nerve cells. The Gabor function has a real and an imaginary component representing orthogonal directions. The two components may be formed into a complex number. A 2D Gabor function can

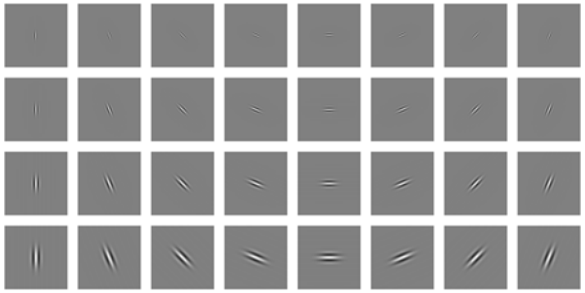

FIGURE 1. Frequency diagram of Gabor filter.

be expressed as (1).

$$g = exp\left(-\frac{x'^2+\gamma^2 y'^2}{2\sigma^2}\right) exp\left(i\left(2\pi\frac{x'}{\lambda}+\psi\right)\right). \quad (1)$$

$$g_{re} = exp\left(-\frac{x'^2+\gamma^2 y'^2}{2\sigma^2}\right) \cos\left(2\pi\frac{x'}{\lambda}+\psi\right). \quad (2)$$

where

$$x' = x\cos\theta + y\sin\theta, y' = -x\sin\theta + y\cos\theta. \quad (3)$$

For the practical application of finger-vein recognition, the real part (g_{re}) of the Gabor function is used. In the Gabor function, λ is the wavelength of the sinusoidal, where $f = \frac{1}{\lambda}$, and f is the frequency of the sinusoidal. θ is the orientation of the normal to the parallel stripes of the Gabor function, ψ is the phase offset, σ is the standard deviation of the Gaussian envelope, γ is the spatial aspect ratio, and it specifies the ellipticity of the Gabor-function support. Fig. 1 shows the frequency diagram of the Gabor filter in eight directions and four scales. The range of θ is $[0, \pi]$, the value of ψ is generally $[0, \pi]$, and γ generally takes the value of 1. Moreover, there is a certain relationship between σ and λ, and its relation expression [43] is (5):

$$b = log_2\left(\frac{\left(\frac{\sigma}{\lambda}+\left(\frac{1}{\pi}\right)\sqrt{\frac{\ln 2}{2}}\right)}{\left(\frac{\sigma}{\lambda}-\left(\frac{\sigma}{\lambda}\right)\sqrt{\frac{\ln 2}{2}}\right)}\right). \quad (4)$$

simplified formula:

$$\sigma = \frac{1}{\pi}\frac{2^b+1}{2^b-1}\sqrt{\frac{\ln 2}{2}}\lambda. \quad (5)$$

where b is the half-response spatial frequency bandwidth of a linear filter.

In the Gabor filter-bank design, the highest frequency, f_m, the total number of frequencies, n_f, and the total number of orientations, n_o, of the Gabor-filter bank is first specified. The combinatorial of the frequency and the orientation are then performed to create the Gabor-filter bank. Example settings of these parameters are shown in Table 1.

TABLE 1. Gabor-filter parameter settings in the literature.

Reference	f_m	n_f	n_o
A.K.Jain et al. [44]	$\sqrt{2}/4$	5	4
S.Li et al. [45]	0.4	4–6	4–6
D.A.Clausi et al. [46]	$\sqrt{2}/4$	4	4
C.Caleanu et al. [47]	0.5	7	8

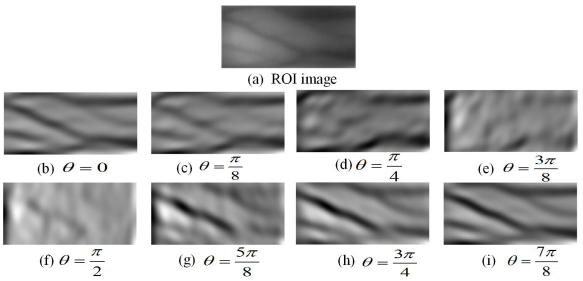

FIGURE 2. Input ROI image and filter responses in different Gabor orientation.

Here, the relationship between f_m, n_f, and n_o can be described as (6) and (7).

$$f_l = a^{-l} f_m, \quad l = 0, 1 \ldots, n_f - 1. \quad (6)$$

$$\theta_\kappa = \kappa\frac{\pi}{n_o}, \quad \kappa = 0, 1 \ldots, n_o - 1. \quad (7)$$

where θ_κ is the κth orientation and n_o is the number of orientations to be used. f_l is the lth frequency, and a is the frequency-scaling factor ($a > 1$).

C. ANALYSISING OF PARAMETERS OF GABOR FUNCTION IN FINGER VEIN

There are three main parameters affecting the waveform in Gabor filters: θ, λ and σ. Finger vein image has clear direction information, vein lines mainly grow along the direction of the finger. If the direction of the finger is horizontal, the veins of the finger are mainly distributed in the horizontal and vertical directions. In order to analyze the direction information of finger vein image, we set different θ values of the Gabor filter. The other parameters are $\lambda = 16, \sigma = 5, \gamma = 1, \psi = 0$. A region of interest (ROI) image of finger vein is filtered by Gabor filters with different θ values to obtain the filtered spectrum, as shown in Fig. 2.

As can be seen from Fig. 2, Gabor filters in different directions can obtain vein lines in different directions, which is consistent with the distribution characteristics of finger vein network analyzed above. More vein information can be obtained by filters biased to the horizontal direction ($\theta = 0$, $\pi/8$, $7\pi/8$) and the vertical direction ($\theta = \pi/2$).

The parameters λ and σ of Gabor function are related to each other. To verify the influence of different λ and σ parameters on finger vein filtering. We set different σ and λ values for Gabor filter. The other parameters are $\theta = 0$, $\gamma = 1$, $\psi = 0$, respectively. An ROI image of finger vein is filtered by the Gabor filter with different σ and λ values, and the filtered spectrum are obtained. As shown in Fig. 3.

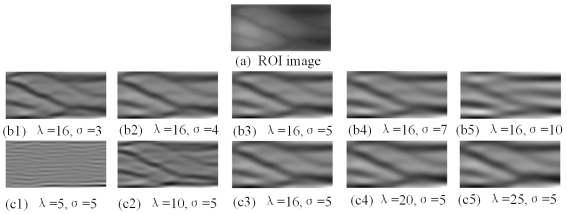

FIGURE 3. Input ROI image and filter responses in different σ and λ.

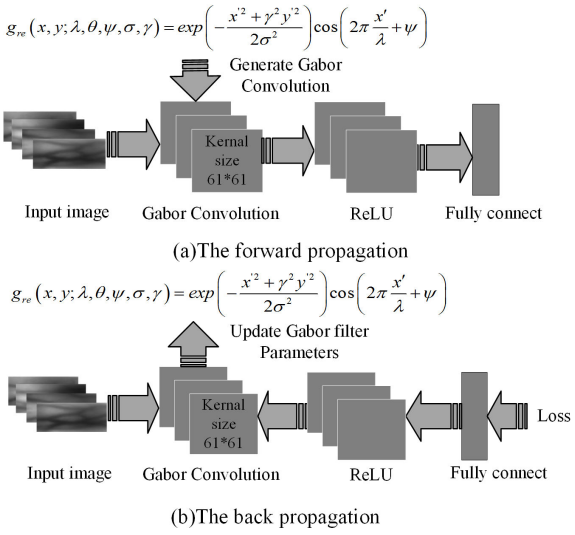

FIGURE 4. Framework of the experiment.

III. OUR METHOD

The framework of the experiment is shown in Fig. 4. The experimental scheme in this paper is mainly based on a CNNs with the ordinary convolution layer replaced by a Gabor convolution layer. In the network structure, the Gabor-filter parameters can be adjusted adaptively. As shown in Fig. 4, our experimental process is divided into two parts: Fig. 4 (a) and Fig. 4 (b).

The forward propagation process is to send the input image into the Gabor convolution layer, the ReLU layer, and the fully-connected layer to reduce the dimension of output features. The back-propagation process updates the parameters of Gabor function by updating the derivation of the parameters according to the objective function, thus realizing the adaptive updating of the parameters of Gabor function.

In our network structure, we use 16 channels of the Gabor convolution layer with sizes 61 $\times$ 61, the ReLU activation function and the fully-connected layer, the final output feature dimension is 128 dimensions, the loss function is softmax, and the optimizer is SGD.

Gabor filter can capture discriminative features not only with more orientations but also with different frequencies. A Gabor filter can be viewed as a sinusoidal plane of particular frequency and orientation, modulated by a Gaussian envelope. According to the nature of the Gabor kernel, the farther the input signal frequency is in the frequency of the Gabor filter kernel, the worse the filtering effect is. Generally, the input frequency should be within 3 σ of the Gabor filter to achieve the best filtering effect. Additionally, the Gabor filter has a larger kernel size, which is beneficial to investigate the structure of the finger vein.

A. CONVOLUTIONAL NEURAL NETWORKS

CNNs [48] are similar to ordinary neural networks: They are made up of neurons that have learnable weights and biases. Each neuron receives inputs, performs a dot product, and optionally follows with a non-linearity. The whole network comprises convolution layer, a pooling layer, an activation layer, a full connection layer, and a loss function.

Stochastic gradient descent [49], also known as incremental gradient descent, is an iterative method for optimizing a differentiable objective function. A stochastic approximation of gradient descent optimization. For each sample, set x^i and y^i, $L\left(\theta; x^i; y^i\right)$ is an objective function, the θ is a parameter that needs to be updated. The formula for updating the parameter θ is:

$$\theta = \theta - \alpha \nabla_\theta L\left(\theta; x^i; y^i\right). \tag{8}$$

where α is a step size, also called ''learning rate''.

We need to update parameters of Gabor function. The back-propagation algorithm [50] is the most common and effective algorithm for training artificial neural networks. Backpropagation is commonly used by the gradient-descent optimization algorithm to adjust the parameters of the Gabor filter by calculating the gradient of the loss function.

Why use CNNs to update the parameters of the Gabor function? Because CNNs has powerful feature extraction capabilities and powerful parameter update capabilities. So we can use CNNs to automatically update the parameters of the Gabor function to solve the problem that the parameters of the Gabor function are difficult to set in the traditional method. And we use the Gabor convolution network with a Gabor convolutional layer, Gabor filter has a good ability to extract features of finger vein texture, and we can achieve good finger vein recognition results based on the characteristics of Gabor filter in smaller data. In this paper, the training of model parameters takes a long time, but when the model training is completed, the parameters of the model are no longer updated. When the finger vein image is processed in real-time, only matrix multiplication and some nonlinear operations are needed. These operations will not affect the speed of real-time processing.

B. UPDATING THE PARAMETERS OF THE GABOR FUNCTION

In our paper, the parameters of each Gabor filter must be optimized. We update the parameters using Back-Propagation and chain rule. The updating formula for parameters [51] are:

$$\frac{\partial g_{re}}{\partial \theta} = \frac{g_{re}x'y'}{\sigma^2}\left(\gamma^2 - 1\right) - G\frac{2\pi y'}{\lambda}. \tag{9}$$

$$\frac{\partial g_{re}}{\partial \lambda} = G\frac{2\pi x'}{\lambda^2}. \tag{10}$$

$$\frac{\partial g_{re}}{\partial \psi} = -G. \tag{11}$$

$$\frac{\partial g_{re}}{\partial \sigma} = g_{re}\frac{x'^2 + \gamma^2 y'^2}{\sigma^3}. \tag{12}$$

$$\frac{\partial g_{re}}{\partial \gamma} = -g_{re}\frac{\gamma y'^2}{\sigma^2}. \tag{13}$$

$$\theta_{t+1} = \theta_t - \alpha\frac{\partial L}{\partial g_{re}}.\frac{\partial g_{re}}{\partial \theta}. \tag{14}$$

$$\lambda_{t+1} = \lambda_t - \alpha\frac{\partial L}{\partial g_{re}}.\frac{\partial g_{re}}{\partial \lambda}. \tag{15}$$

$$\psi_{t+1} = \psi_t - \alpha\frac{\partial L}{\partial g_{re}}.\frac{\partial g_{re}}{\partial \psi}. \tag{16}$$

$$\sigma_{t+1} = \sigma_t - \alpha\frac{\partial L}{\partial g_{re}}.\frac{\partial g_{re}}{\partial \sigma}. \tag{17}$$

$$\gamma_{t+1} = \gamma_t - \alpha\frac{\partial L}{\partial g_{re}}.\frac{\partial g_{re}}{\partial \gamma}. \tag{18}$$

where

$$G = exp\left(-\frac{x'^2 + \gamma^2 y'^2}{2\sigma^2}\right)\sin\left(2\pi\frac{x'}{\lambda} + \psi\right). \tag{19}$$

L is the objective function. α is a step size, also called 'learning rate'.

IV. IMPLEMENTATION AND EXPERIMENTS

A. DATABASE INTRODUCTION

MMCBNU_6000 [52] is a public database of finger vein images, founded by 100 volunteers from 20 countries. A collection for each of the six fingers is repeated 10 times to obtain 60 finger-vein images for each volunteer. Hence, MMCBNU_6000 comprises 6,000 images. Each image is stored in a.BMP format with a resolution of 480 × 640. The ROI images that are provided by the database are utilized in this paper. The size of each image is 60 × 128. There were 4, 800 training images, 8 images per each finger, 1, 200 test images, and 2 images per each finger.

The FV-USM database [53] is a finger vein database which is from University Sains Malaysia. FV-USM consists of 2, 952 BMP images with 640 × 480 resolution, taken from 123 subjects with 4 fingers per subject. Images have been acquired in two different sessions with six images per finger in every session. There were 1, 968 training images, 4 images per each finger, 984 test images, 2 images per each finger. The ROI images that are provided by the database are utilized in this paper.

The SDUMLA database [54] is a finger vein database which is form Shandong University of China. SDUMLA consists of 3, 816 BMP images with 320 × 240 resolution, taken from 106 subjects with 6 fingers per subject. There were 2, 544 training images, 4 images per each finger, 1, 272 test images and 2 images per each finger. The ROI image is obtained by processing in literature [55].

The Hong kong Polytechnic University finger vein database (HKPU) [56] is captured from 156 volunteers. It consists of 3, 132 finger vein images with 513 × 256 resolution from the middle finger and index finger. In this database, the first session contains 210 fingers with 12 images per finger; the second session contains 102 fingers with 6 images per finger. In order to compare objectively with the existing methods, we use the data of the first session to train the parameters, and the data of the second session to evaluate the recognition performance of our proposed methods. The ROI image is obtained by processing in literature [56].

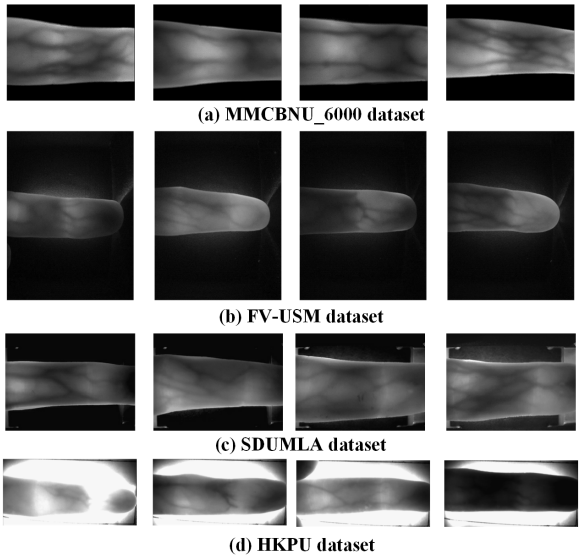

FIGURE 5. Some images of different finger vein datasets.

To objectively compare with the existing finger vein recognition methods, we adopt the same test protocol as that in the literature [20]. In the multiple templates test protocol, one image per finger of test dataset is selected as the probe, and the all images per finger of training dataset are used as the enrolled templates, which is repeated and the average performance is reported. In the second session of HKPU database, one image per finger is selected as the probe, and others of per finger are used as the enrolled templates, which is repeated and the average performance is reported. Such as SDUMLA database, four images per finger of training dataset are selected as the enrolled templates, and all images per finger of test dataset are used as the probe. So the genuine matches are 1,272 matches, and the imposter matches are $1272 \times 635 = 807720$ matches.

Fig. 5 displays some finger-vein images of different finger vein datasets. Some ROI images of different finger vein datasets are shown in Fig. 6.

B. LEARNING OF MAIN ORIENTATION OF THE GABOR FILTER

For finger-vein recognition, the Gabor filter with parameter θ can capture the vein-image texture direction information very well. This experiment is divided into two types. First, the experimental data is the original ROI images of the MMCBNU_6000 dataset. This experiment proves that the parameter θ of the Gabor function is adaptively learned.

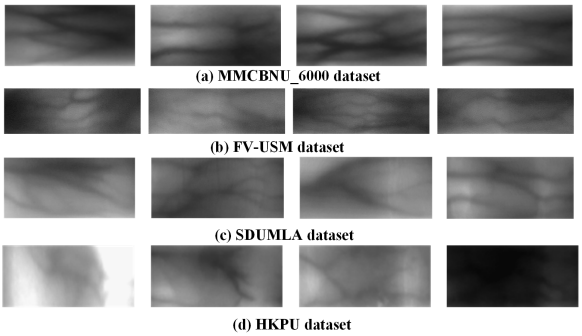

FIGURE 6. Some ROI images of different finger vein datasets.

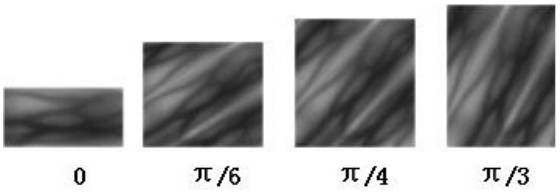

FIGURE 7. Images with different rotation angles and mirror fill.

Second, the experimental data is the original ROI image of the MMCBNU_6000 dataset as first expanded by a mirror, then rotated $\pi/6$, $\pi/4$, and $\pi/3$. Fig. 7 shows finger-vein images with different rotation angles and mirror fill.

The rotated image contains all the information of the original ROI image, ensuring that the original ROI image information is not lost and that the boundary problem caused by rotation is not introduced. This experiment proves that the parameter θ of the Gabor function can be self-adaptive for different rotation angle data.

Initialization settings of the parameters of the Gabor function: $\lambda = 16$, $\theta \in [0, \pi]$, $\sigma = 5$, $\psi = 0$, $\gamma = 1$, 16 Gabor convolutions (Gabor filter), the convolution size is 61×61. In this experiment, the learning rate of parameter θ of the Gabor function is set to 0.1, and the learning rate of other parameters of the Gabor function is set to 0. Thus, the experiment updates only parameter θ of the Gabor function. First, the experimental data are the original ROI images. The results of the experiment are shown in Fig. 8(a).

As can be seen from Fig. 6, the finger-vein image has clear directional information, and it grows along the horizontal direction of the finger. As can be seen from Fig. 8(a), parameter θ of the Gabor function converges mainly near the angles of 0, $\pi/2$, and π. Most of θ converges near 0 and π. A few theta converge to $\pi/2$. Moreover, the vein texture of the finger is mainly horizontal and vertical, which is consistent with the parameter θ of the Gabor function, adaptively learned. Experiments prove that the parameter θ of the Gabor function can converge to the optimal value via adaptive learning.

To further prove that the parameter θ of the Gabor function can be self-adaptive, we repeat the above experiments by rotating the original ROI image. The experimental data is the original ROI image, first expanded by a mirror, and then rotated $\pi/6$, $\pi/4$, and $\pi/3$. The results of the experiment are shown in Fig. 8(b)-(d).

As can be seen from Fig. 8(b)-(d), with the image rotation at different angles, the parameter θ can finally learn the texture changes of the image. Parameter θ of the Gabor function eventually converges to the texture direction of the rotating image. This experiment further proves that the parameter θ of the Gabor function can be adjusted adaptively.

C. LEARNING PARAMETERS λ AND σ OF GABOR FILTER

In this experiment, the parameter σ of the Gabor filter is fixed between [4, 10], and the step size is 1. We study the parameter λ of the Gabor filter and observe the change of λ and the relationship between parameter λ and parameter σ.

The initialization settings of the Gabor filter are $\lambda \in [30, 35]$, $\theta = 0$, $\psi = 0$, $\gamma = 1$, and 16 Gabor convolutions, and the convolution size is 61×61. In this experiment, the learning rate of parameter λ of the Gabor function is set to 0.01, and the learning rate of other parameters is set to 0. Thus, the experiment updates the parameter λ of the Gabor function only. The experimental data is the ROI image of the MMCBNU_6000 dataset. The experimental flow is shown in Fig. 4. The results of our experiments that selected several different sigma values are shown in Fig. 9.

Under a different parameter, σ, we study parameter λ of the Gabor function, which converges in a small interval. The accuracy of the test set and the relationship between parameter λ and parameter σ are shown in Table 2.

Based on the analysis of Fig. 9 and Table 2, when parameter σ of the Gabor function is 4 to 10, the parameter λ of the Gabor function can converge to a relatively suitable interval. Then, there is a certain relationship between parameter σ and λ. The relationship is shown in (5).

Analyzing the values of σ and λ in Table 2, we get

$$\frac{\sigma}{\lambda} \in [0.27, 0.39]. \tag{20}$$

By analyzing Table 2, the parameters σ and λ of the Gabor function are a pair of combinations. From the process of learning the parameters of the Gabor functions, prior knowledge of σ and λ can be directly added. In this experiment, we analyze the experiment of the self-learning adjustment of parameters of the Gabor function. There is a certain relationship between λ and σ, which is related to the bandwidth of the signal. The frequency information of the data can be analyzed to determine the bandwidth information. Therefore, the relationship between σ and λ can be calculated, and σ changes with λ. By changing parameter λ of the Gabor function, we can change the parameter σ of the Gabor function.

D. COMPARISON WITH THE STATE-OF-THE-ART ALGORITHMS

In this section, the five parameters of the Gabor function can be learned and updated. And the performance of our method, compared with the state-of-the-art finger vein recognition

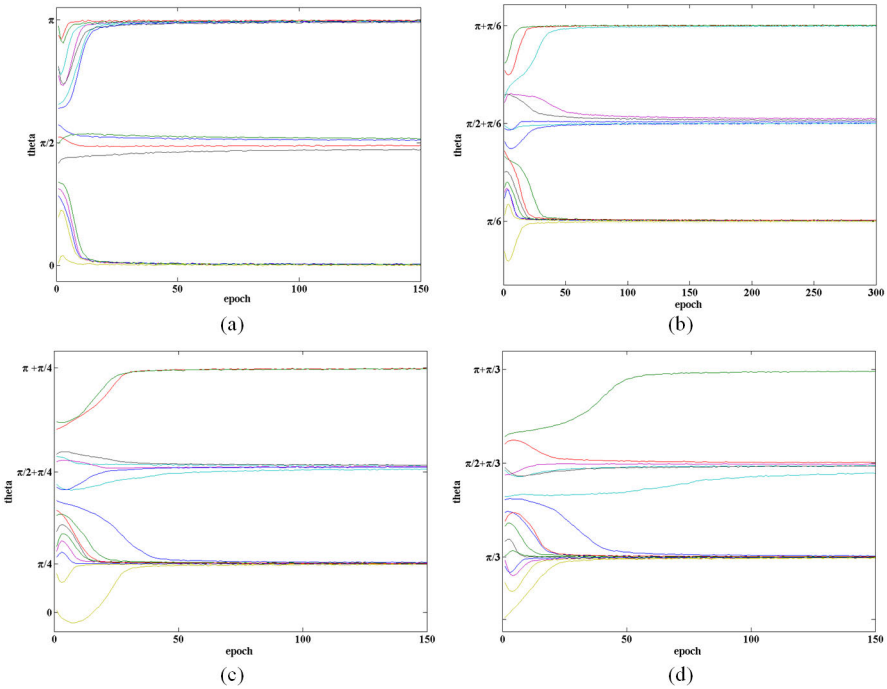

FIGURE 8. The θ change curve of 16 Gabor function in ROI images. (a) original ROI images; (b) $\pi/6$ rotation; (c) $\pi/4$ rotation; (d) $\pi/3$ rotation.

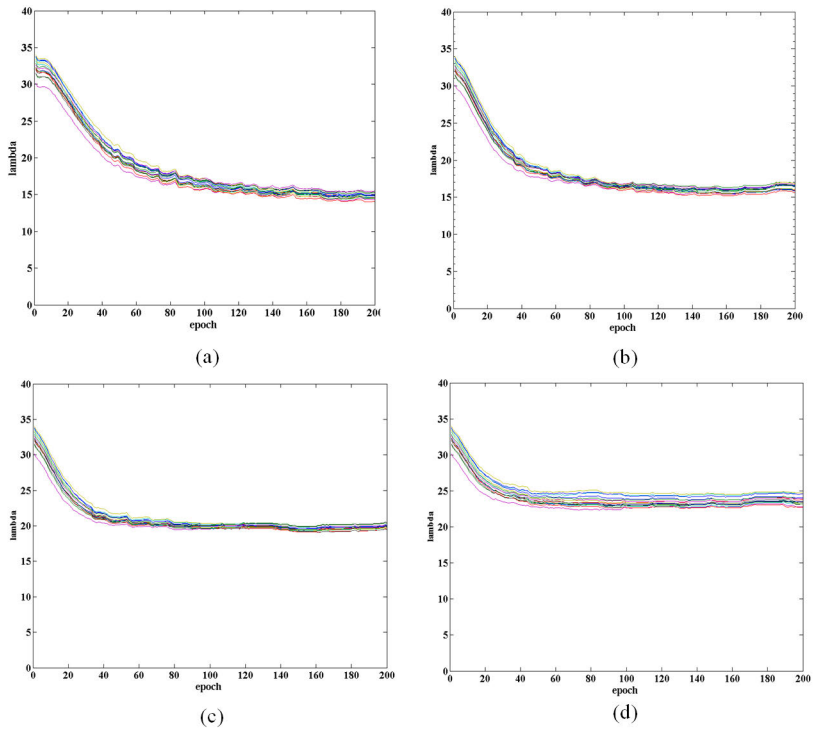

FIGURE 9. The λ change curve of Gabor function. (a) $\sigma = 4$;(b) $\sigma = 5$;(c)$\sigma = 7$;(d)$\sigma = 9$.

algorithms on four public finger vein databases, is presented in Tables 3-6.

As we can see from Tables 3-5, we compare our proposed adaptive Gabor filter method with other Gabor methods, such as Gabor filter, Gabor+Tri-branch structure [19], PG-Gabor [20], our method has better performance than other Gabor methods. This proves that our method can update the parameters of Gabor function better and extract the main

TABLE 2. The accuracy of test set and the relationship between λ and σ.

σ	Mean of λ	Accuracy of test set	$\frac{\sigma}{\lambda}$
4	14.56	98.92%	0.275
5	16.04	99.16%	0.312
6	18.03	99.08%	0.333
7	20.07	98.92%	0.349
8	22.11	98.92%	0.362
9	23.80	98.75%	0.378
10	25.76	98.50%	0.388

TABLE 3. Comparison with the state-of-the-art methods on MMCBNU_6000 database.

Method	Year	EER%
Gabor filters [56]		2.42
Repeated line tracking [20]		5.74
Maximum curvature [20]		2.69
KMHM [28]	2017	2.08
ITQM [29]	2017	1.33
Gabor+Tri-branch structure [19]	2017	1.14
Combining primary and soft biometric traits [57]	2019	0.82
PG-Gabor [20]	2019	0.71
Weighted Vein code indexing [30]	2019	0.42
Our method	2019	0.11

TABLE 4. Comparison with the state-of-the-art methods on FV-USM database.

Method	Year	EER%
Gabor filters [57]		4.75
KMHM [28]	2017	5.41
ITQM [29]	2017	1.05
Deep representation-based feature extraction [36]	2017	1.69
Combining primary and soft biometric traits [57]	2019	0.22
Weighted Vein code indexing [30]	2019	0.07
Our method	2019	0.57

TABLE 5. Comparison with the state-of-the-art methods on SDUMLA database.

Method	Year	EER%
LLBP [31]		2.65
Repeated line tracking [20]		5.85
Maximum curvature [20]		3.65
Gabor filters [57]		2.58
KMHM [28]	2017	4.97
ITQM [29]	2017	2.78
Gabor+Tri-branch structure [19]	2017	4.04
PG-Gabor [20]	2019	1.35
Weighted Vein code indexing [30]	2019	0.99
Combining primary and soft biometric traits [57]	2019	0.72
Our method	2019	1.09

vein information of finger vein image. And our method has the best performance compared with other latest methods and other classical methods, such as k-means hashing-based method (KMHM) [28], iterative quantization-based method (ITQM) [29], Deep representation-based feature extraction [36], Repeated line tracking, Maximum curvature, LLBP, ELBP. However, compared with Combining primary and soft biometric traits [57], Weighted Vein code indexing [30], our method performs worse on SDUMAL and FV-USM datasets. The main reason is that [57] combines

TABLE 6. Comparison with the state-of-the-art methods on second session of HKPU database.

Method	Year	EER%
Gabor [56]		4.61
Fusion-based method [58]	2015	4.47
ELBP [25]	2016	5.59
Deep representation-based feature extraction [36]	2017	3.02
ASAVE [31]	2018	2.91
Weighted Vein code indexing [30]	2019	3.33
Our method	2019	1.67

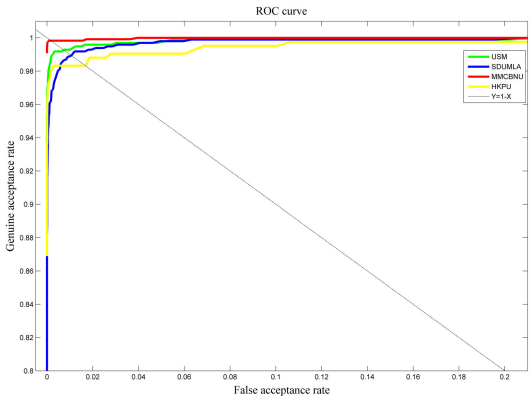

FIGURE 10. Comparisons of ROC curves of the proposed method on different finger vein databases.

primary and soft biometric traits to increase the amount of information and [30] has a question of high complexity. But our method is an end-to-end learning method and can extract the original features of the image. Table 6 shows the results of the test in an open-world setting. We use the first session of the HKPU dataset to train and test in the second session. The classes of training data and test data belong to different classes. The experimental results also demonstrate the effectiveness of the proposed method. Figure 10 shows the comparison of the ROC curves of the proposed method on different finger vein datasets. On the whole, our method focuses more on solving the problem of Gabor parameters being difficult to tune. Moreover, the performance of the proposed method is comparable to that of the latest finger vein recognition methods.

V. CONCLUSION

We proposed an adaptive Gabor filter to solve the problem where its parameters are difficult to adjust. First, we showed how to reformulate the Gabor convolution and gradient descent into a consolidated architecture of filtering and optimization. Second, parameter θ of the Gabor filter represented the directional information, having little correlation with other parameters. Experiments prove that parameter θ could be learned independently and the recognition performance of the finger vein was superior to the general Gabor method. Third, parameter σ had a certain relationship with parameter λ, and parameter λ of the Gabor filter well-converged to the optimal value. So we could choose the better Gabor-filter parameters and apply the prior relationship of parameters in

the design of the Gabor filter bank. Finally, experimental results show that our method achieved a good performance on four finger vein datasets. This performance was superior to other Gabor methods and our method outperforms state-of-the-art methods in finger-vein classification.

In the future. we are going to design an adaptive Gabor convolution neural network, where the weights of convolution have information of direction and spatial frequency. And we will also combine the soft features of the finger veins to improve the performance of recognition.

REFERENCES

[1] J.-D. Wu and S.-H. Ye, "Driver identification using finger-vein patterns with Radon transform and neural network," *Expert Syst. Appl.*, vol. 36, no. 3, pp. 5793–5799, Apr. 2009.

[2] L. Wang, G. Leedham, and S. Gho, "Infrared imaging of hand vein patterns for biometric purposes," *IET Comput. Vis.*, vol. 1, no. 3, pp. 113–122, Dec. 2007.

[3] M. Farmanbar and Ö. Toygar, "A hybrid approach for person identification using palmprint and face biometrics," *Int. J. Pattern Recognit. Artif. Intell.*, vol. 29, no. 6, Sep. 2015, Art. no. 1556009.

[4] J. Climent and R. A. Hexsel, "Iris recognition using AdaBoost and levenshtein distances," *Int. J. Pattern Recognit. Artif. Intell.*, vol. 26, no. 2, Mar. 2012, Art. no. 1266001.

[5] M. P. Down and R. J. Sands, "Biometrics: An overview of the technology, challenges and control considerations," *Inf. Syst. Control J.*, vol. 4, pp. 53–56, 2004.

[6] D. T. Nguyen, Y. H. Park, K. Y. Shin, S. Y. Kwon, H. C. Lee, and K. R. Park, "Fake finger-vein image detection based on Fourier and wavelet transforms," *Digital Signal Process.*, vol. 23, no. 5, pp. 1401–1413, Sep. 2013.

[7] D. Menotti, L. Najman, J. Facon, and A. D. A. Araujo, "Multi-histogram equalization methods for contrast enhancement and brightness preserving," *IEEE Trans. Consum. Electron.*, vol. 53, no. 3, pp. 1186–1194, Aug. 2007.

[8] S. Shazeeda and B. A. Rosdi, "Finger vein recognition using mutual sparse representation classification," *IET Biometrics*, vol. 8, no. 1, pp. 49–58, Jan. 2018.

[9] R. Wang, G. Wang, Z. Chen, Z. Zeng, and Y. Wang, "A palm vein identification system based on Gabor wavelet features," *Neural Comput. Appl.*, vol. 24, no. 1, pp. 161–168, Jan. 2014.

[10] M. Kaur and G. Babbar, "Finger vein detection using repeated line tracking, even Gabor and multilinear discriminant analysis (MDA)," *Int. J. Comput. Sci. Inf. Technol.*, vol. 6, no. 4, pp. 3280–3284, 2015.

[11] J. Yang, J. Yang, and Y. Shi, "Finger-vein segmentation based on multi-channel even-symmetric Gabor filters," in *Proc. IEEE Int. Conf. Intell. Comput. Intell. Syst.*, Shanghai, China, Nov. 2009, pp. 500–503.

[12] J. Yang, Y. Shi, and J. Yang, "Finger-vein recognition based on a bank of gabor filters," in *Computer Vision—ACCV*, vol. 5994, H. Zha, R. Taniguchi, and S. Maybank, Eds. Berlin, Germany: Springer, 2010, pp. 374–383.

[13] J. Zhang and J. Yang, "Finger-vein image enhancement based on combination of gray-level grouping and circular Gabor filter," in *Proc. Int. Conf. Inf. Eng. Comput. Sci.*, Wuhan, China, Dec. 2009, pp. 1–4.

[14] J. Yang and J. Yang, "Multi-channel Gabor filter design for finger-vein image enhancement," in *Proc. 5th Int. Conf. Image Graph.*, Xi'an, China, Sep. 2009, pp. 87–91.

[15] M. A. Ferrer, A. Morales, and L. Ortega, "Infrared hand dorsum images for identification," *Electron. Lett.*, vol. 45, no. 6, pp. 306–308, Mar. 2009.

[16] Y. Shi and J. Yang, "Image restoration and enhancement for finger-vein recognition," in *Proc. IEEE 11th Int. Conf. Signal Process.*, Beijing, China, Oct. 2012, pp. 1605–1608.

[17] S. J. Xie, J. Yang, S. Yoon, L. Yu, and D. S. Park, "Guided Gabor filter for finger vein pattern extraction," in *Proc. 8th Int. Conf. Signal Image Technol. Internet Based Syst.*, Naples, Italy, Nov. 2012, pp. 118–123.

[18] Y. Lu, S. Yoon, S. J. Xie, J. Yang, Z. Wang, and D. S. Park, "Finger vein recognition using histogram of competitive Gabor responses," in *Proc. 22nd Int. Conf. Pattern Recognit.*, Stockholm, Sweden, Aug. 2014, pp. 1758–1763.

[19] L. Yang, G. Yang, X. Xi, X. Meng, C. Zhang, and Y. Yin, "Tri-branch vein structure assisted finger vein recognition," *IEEE Access*, vol. 5, pp. 21020–21028, 2017.

[20] L. Yang, G. Yang, K. Wang, H. Liu, X. Xi, and Y. Yin, "Point grouping method for finger vein recognition," *IEEE Access*, vol. 7, pp. 28185–28195, 2019.

[21] N. Miura, A. Nagasaka, and T. Miyatake, "Feature extraction of finger vein patterns based on iterative line tracking and its application to personal identification," *Syst. Comput. Jpn.*, vol. 35, no. 7, pp. 61–71, Jun. 2004.

[22] N. Miura, A. Nagasaka, and T. Miyatake, "Extraction of finger-vein patterns using maximum curvature points in image profiles," *IEICE Trans. Inf. Syst.*, vol. E90-D, no. 8, pp. 1185–1194, Aug. 2007.

[23] E. C. Lee, H. C. Lee, and K. R. Park, "Finger vein recognition using minutia-based alignment and local binary pattern-based feature extraction," *Int. J. Imag. Syst. Technol.*, vol. 19, no. 3, pp. 179–186, Sep. 2009.

[24] B. A. Rosdi, W. S. Chai, and S. A. Suandi, "Finger vein recognition using local line binary pattern," *Sensors*, vol. 11, no. 12, pp. 11357–11371, Nov. 2011.

[25] C. Liu and Y.-H. Kim, "An efficient finger-vein extraction algorithm based on random forest regression with efficient local binary patterns," in *Proc. Int. Conf. Image Process. (ICIP)*, Phoenix, AZ, USA, Sep. 2016, pp. 3141–3145.

[26] X. Xi, L. Yang, and Y. Yin, "Learning discriminative binary codes for finger vein recognition," *Pattern Recognit.*, vol. 66, pp. 26–33, Jun. 2017.

[27] H. Liu, L. Yang, G. Yang, and Y. Yin, "Discriminative binary descriptor for finger vein recognition," *IEEE Access*, vol. 6, pp. 5795–5804, 2018.

[28] K. Su, G. Yang, L. Yang, and Y. Yin, "Finger vein image retrieval via affinity-preserving K-means hashing," in *Proc. IEEE Int. Joint Conf. Biometrics (IJCB)*, Denver, CO, USA, Oct. 2017, pp. 375–382.

[29] K. Wang, L. Yang, G. Yang, and Y. Yin, "Integration of discriminative features and similarity-preserving encoding for finger vein image retrieval," in *Proc. IEEE Int. Conf. Image Process. (ICIP)*, Beijing, China, Sep. 2017, pp. 3525–3529.

[30] L. Yang, G. Yang, X. Xi, K. Su, Q. Chen, and Y. Yin, "Finger vein code: From indexing to matching," *IEEE Trans. Inf. Forensics Security*, vol. 14, no. 5, pp. 1210–1223, May 2019.

[31] L. Yang, G. Yang, Y. Yin, and X. Xi, "Finger vein recognition with anatomy structure analysis," *IEEE Trans. Circuits Syst. Video Technol.*, vol. 28, no. 8, pp. 1892–1905, Aug. 2018.

[32] S. A. Radzi, M. K. Hani, and R. Bakhteri, "Finger-vein biometric identification using convolutional neural network," *Turkish J. Electr. Eng. Comput. Sci.*, vol. 24, no. 3, pp. 1863–1878, 2016.

[33] C. Xie and A. Kumar, "Finger vein identification using convolutional neural network and supervised discrete hashing," *Pattern Recognit. Lett.*, vol. 119, pp. 148–156, Mar. 2019.

[34] Y. Fang, Q. Wu, and W. Kang, "A novel finger vein verification system based on two-stream convolutional network learning," *Neurocomputing*, vol. 290, pp. 100–107, May 2018.

[35] E. Jalilian and A. Uhl, "Finger-vein recognition using deep fully convolutional neural semantic segmentation networks: The impact of training data," in *Proc. IEEE Int. Workshop Inf. Forensics Secur. (WIFS)*, Hong Kong, Dec. 2018, pp. 1–8.

[36] H. Qin and M. A. El-Yacoubi, "Deep representation-based feature extraction and recovering for finger-vein verification," *IEEE Trans. Inf. Forensics Security*, vol. 12, no. 8, pp. 1816–1829, Aug. 2017.

[37] D. Gabor, "Theory of communication," *J. Inst. Elect. Eng.*, vol. 93, no. 3, pp. 429–457, 1946.

[38] J. G. Daugman, "Two-dimensional spectral analysis of cortical receptive field profiles," *Vis. Res.*, vol. 20, no. 10, pp. 847–856, Jan. 1980.

[39] S. Marĉelja, "Mathematical description of the responses of simple cortical cells," *J. Opt. Soc. Amer.*, vol. 70, no. 11, pp. 1297–1300, Nov. 1980.

[40] D. A. Pollen and S. F. Ronner, "Visual cortical neurons as localized spatial frequency filters," *IEEE Trans. Syst., Man, Cybern. Syst.*, vol. SMC-13, no. 5, pp. 907–916, Sep. 1983.

[41] J. G. Daugman, "Complete discrete 2-D Gabor transforms by neural networks for image analysis and compression," *IEEE Trans. Acoust., Speech Signal Process.*, vol. 36, no. 7, pp. 1169–1179, Jul. 1988.

[42] M. Porat and Y. Y. Zeevi, "The generalized Gabor scheme of image representation in biological and machine vision," *IEEE Trans. Pattern Anal. Mach. Intell.*, vol. 10, no. 4, pp. 452–468, Jul. 1988.

[43] J. G. Daugman, "Uncertainty relation for resolution in space, spatial frequency, and orientation optimized by two-dimensional visual cortical filters," *J. Opt. Soc. Amer. A, Opt. Image Sci.*, vol. 2, no. 7, pp. 1160–1169, Jul. 1985.

[44] A. K. Jain and F. Farrokhnia, "Unsupervised texture segmentation using Gabor filters," *Pattern Recognit.*, vol. 24, no. 12, pp. 1167–1186, 1991.
[45] S. Li and J. Shawe-Taylor, "Comparison and fusion of multiresolution features for texture classification," *Pattern Recognit. Lett.*, vol. 26, no. 5, pp. 633–638, Apr. 2005.
[46] D. A. Clausi and H. Deng, "Design-based texture feature fusion using Gabor filters and co-occurrence probabilities," *IEEE Trans. Image Process.*, vol. 14, no. 7, pp. 925–936, Jul. 2005.
[47] C. Căleanu, D.-S. Huang, V. Gui, V. Tiponuţ, and V. Maranescu, "Interest operator versus Gabor filtering for facial imagery classification," *Pattern Recognit. Lett.*, vol. 28, no. 8, pp. 950–956, Jun. 2007.
[48] Y. LeCun, B. Boser, J. S. Denker, D. Henderson, R. E. Howard, W. Hubbard, and L. D. Jackel, "Backpropagation applied to handwritten zip code recognition," *Neural Comput.*, vol. 1, no. 4, pp. 541–551, 1989.
[49] Y. Tsuruoka, J. Tsujii, and S. Ananiadou, "Stochastic gradient descent training for L1-regularized log-linear models with cumulative penalty," in *Proc. Joint Conf. 47th Annu. Meeting ACL 4th Int. Joint Conf. Natural Lang. Process. (AFNLP)*, Singapore, vol. 1, 2009, pp. 477–485.
[50] D. E. Rumelhart, G. E. Hinton, and R. J. Williams, "Learning representations by back-propagating errors," *Nature*, vol. 323, no. 6088, pp. 533–536, 1986, doi: 10.1038/323533a0.
[51] Y. Zhang, W. Li, L. Zhang, and Y. Lu, "Adaptive Gabor convolutional neural networks for finger-vein recognition," in *Proc. Int. Conf. High Perform. Big Data Intell. Syst. (HPBD&IS)*, Shenzhen, China, May 2019, pp. 219–222, doi: 10.1109/HPBDIS.2019.8735471.
[52] Y. Lu, S. J. Xie, S. Yoon, Z. Wang, and D. S. Park, "An available database for the research of finger vein recognition," in *Proc. 6th Int. Congr. Image Signal Process. (CISP)*, Hangzhou, China, Dec. 2013, pp. 410–415.
[53] M. S. M. Asaari, S. A. Suandi, and B. A. Rosdi, "Fusion of band limited phase only correlation and width centroid contour distance for finger based biometrics," *Expert Syst. Appl.*, vol. 41, no. 7, pp. 3367–3382, Jun. 2014.
[54] Y. Yin, L. Liu, and X. Sun, "SDUMLA-HMT: A multimodal biometric database," in *Proc. 6th Chin. Conf. Biometric Recognit.*, Beijing, China, Dec. 2011, pp. 260–268.
[55] L. Yang, G. Yang, L. Zhou, and Y. Yin, "Superpixel based finger vein ROI extraction with sensor interoperability," in *Proc. Int. Conf. Biometrics (ICB)*, Phuket, Thailand, May 2015, pp. 444–451.
[56] A. Kumar and Y. Zhou, "Human identification using finger images," *IEEE Trans. Image Process.*, vol. 21, no. 4, pp. 2228–2244, Apr. 2012.
[57] W. Kang, Y. Lu, D. Li, and W. Jia, "From noise to feature: Exploiting intensity distribution as a novel soft biometric trait for finger vein recognition," *IEEE Trans. Inf. Forensics Security*, vol. 14, no. 4, pp. 858–869, Apr. 2019.
[58] P. Gupta and P. Gupta, "An accurate finger vein based verification system," *Digit. Signal Process.*, vol. 38, pp. 43–52, Mar. 2015.

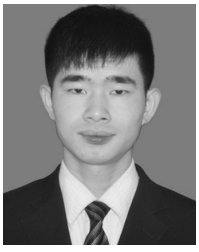

YAKUN ZHANG received the B.E. degree from the Department of Physics, Taiyuan University of Technology, China, in 2015. He is currently pursuing the Ph.D. degree with the Institute of Semiconductors, Chinese Academy of Sciences. His main research interests include biometrics and deep learning.

WEIJUN LI received the Ph.D. degree from the Institute of Semiconductors, Chinese Academy of Sciences, in 2004. He is currently a Professor of artificial intelligence with the Institute of Semiconductors, Chinese Academy of Sciences (ISCAS), and the University of Chinese Academy of Sciences. He is in charge of the Artificial Intelligence Research Center, ISCAS and the Director of the Laboratory of High-Speed Circuits and Neural Networks, ISCAS. His research interests include deep modeling, machine art, pattern recognition, artificial neural networks, and intelligent systems.

LIPING ZHANG received the Ph.D. degree from the Institute of Semiconductors, Chinese Academy of Sciences, in 2018. She is currently an Assistant Research Fellow with the Laboratory of High-Speed Circuit and Artificial Neural Networks, Institute of Semiconductors, Chinese Academy of Sciences. Her research interests include pattern recognition, machine learning, and deep modeling.

XIN NING received the Ph.D. degree from the Institute of Semiconductors, Chinese Academy of Sciences, in 2017. He is currently an Assistant Professor of artificial intelligence with the Institute of Semiconductors, Chinese Academy of Sciences. His research interests include deep learning machine art, pattern recognition, and image cognitive computation.

LINJUN SUN received the B.E. degree from the School of Physics, Huazhong University of Science and Technology, China, in 2013. He is currently pursuing the Ph.D. degree with the Institute of Semiconductors, Chinese Academy of Sciences. His main research interests include computer vision and deep learning.

YAXUAN LU received the B.E. degree from the School of Materials Science and Engineering, Hebei University of Technology, China, in 2015. She is currently pursuing the Ph.D. degree with the Institute of Semiconductors, Chinese Academy of Sciences. Her main research interests include computer vision and deep learning.